Soot Investigation on Fish Oil Spray Combustion in a Constant Volume Cell

M. Malin, V. Krivopolianskii, B.M. Rygh, V. Aesoy, E. Pedersen

Abstract

Maritime environmental regulations stipulate lower emissions from the shipping industry. To cope with these rules, improving the combustion processes, make use of cleaner alternative fuels and implement exhaust gas cleaning systems is necessary. Alternative fuels, like fish oil, have a potential to reduce soot formation during the combustion process and will be deeply investigated in this paper. For this purpose, two different types of fish oil and their blends with marine gas oil (MGO) have been tested in a constant volume pre-combustion cell (CVPC). The CVPC laboratory was built in collaboration between MARINTEK and NTNU. To generate similar injection condition in the combustion cell as in an internal combustion engine, the CVPC is heated using a chemical heating process. The CVPC is used as a fundamental investigation tool for studying the fuel injection system for large engine applications. Parameters that were studied include the combustion, spray development, fuel evaporation process and ignition delay. The general experimental setup of the test facility is described and the optical methods applied are explained for the investigation of fish oil. The aim is to study soot intensity and spray development and to compare the results to pure low-sulphur MGO as a reference fuel. The results conclude that the combustion and ignition properties of fish oil are very similar to marine gas oil and this makes it applicable as an alternative fuel for power generation in the maritime industry. The tests also showed a significant decrease in soot formation for the two fish oils.

Introduction

As the earth's population and peoples standard of living increases, the global society is faced with an increasing energy demand. Fossil fuels have been a reliable source of energy in the past and will continue to be an important energy source in the future. However, fossil energy sources are finite and new energy sources must be investigated to ensure energy security in the future.

Biologically derived fuels have the advantage of being produced from organic material and are hence renewable. Biofuels are also carbon neutral and their use will prevent further build-up of carbon dioxide in the atmosphere. The marine industry is in these days facing stricter emission regulations and the introduction of new and expansion of existing emission controlled areas means that the industry will be needing cleaner fuels. As cleaner more refined petroleum products are expensive, biofuels can be an economically viable alternative.

Biofuel shows positive effects on greenhouse gas (GHG) emissions, but based on the production pathway the magnitude of savings are varying. A Well-To-Wheel (WTW) analysis conducted by the European Environment Agency in 2006 [1] shows GHG emission savings in the range of 50% - 90% and an analysis done by the European Commission in 2011 [2] conclude with savings in the range of 40% - 70%.

Studies on emission characteristics from the combustion of biodiesel are well documented and there seems to be an established consensus of the positive and negative impact biofuels have on emission characteristics. The main difference in chemical structure between biodiesel and petroleum diesel are the fuel bound oxygen found in the ester group of the biodiesel. This oxygen is believed to be the main reason for differences in emission characteristics. Increased oxygen content promotes the mixing process leading to a cleaner, more complete, combustion, which reduces the emissions of unburned hydrocarbons [3]. More oxygen also facilitates oxidation of carbon to carbon monoxide and further to carbon dioxide. This decreases the emissions of soot and carbon monoxide. The soot emissions are further decreased by the biofuels lack of aromatics, which is believed to be the origin of polycyclic aromatic hydrocarbons, also causing soot emissions [4]. In addition, emissions of sulphur oxides are eliminated due to the biofuels lack of sulphur. However, emissions of nitrogen oxides are believed to increase [5], [6], [7] and the heating value is reduced. This is also contributed to the increased oxygen content. The increased oxygen content improves the combustion process leading to a higher combustion temperature, which facilitates the oxidation of nitrogen. The oxygen also occupies volume otherwise used by hydrocarbons and these results in the biofuels lower energy content compared to petroleum diesel.

Two different biofuels and their blends (in sum six fuels) based on fish waste are tested in this study. One is an unprocessed crude fish oil (CFO) produced from category two aquatic products. Category two aquatic products is farmed fish that has died or been killed for other reasons than human consumption. The main problem with this fuel is the high viscosity and low volatility compared to petroleum diesel [8]. For these reasons, the other biofuel is processed through transesterification of fish oil to produce a biofuel with similar viscosity and volatility as petroleum diesel. Fatty acid oils contain triglycerides, which are esters that consist of one glycerol molecule and three fatty acid molecules. In the transesterification process, the oil is reacted

with alcohol and a catalyst and the fatty acid molecules breaks of the glycerol molecule. Each of these fatty acid molecules then bonds with one alcohol molecule to form a fatty acid alkyl ester. The overall carbon atoms per fatty acid molecule will reduce and this lowers the viscosity [9]. In our case, ethanol is the alcohol used and hence is the biofuel a fatty acid ethyl ester (FAEE). Marine gas oil (MGO) is used as the baseline fuel and as the base for the different blends.

To use biofuels in the right way and to gain an advantage, it is necessary to understand the complex diffusion combustion occurring during the fuel injection. The knowledge of spray characteristic of biodiesel and blends with petroleum diesel is so far limited and especially for biofuel derived from fish. A closer study of blended fuels is important since biofuel will not be used pure in most application. It will be, and it is, used as a blend with petroleum diesel. In this study a constant volume pre-combustion cell (CVPC) has been used to study spray characteristics and the broadband radiation (intensity) during combustion of the two fish oils in blends with MGO. By analyzing the intensity, it is possible to determine qualitatively the soot formation when combusting different fuels. Both CFO and FAEE have been investigated. Because of the high viscosity of CFO it was necessary to blend 50% CFO with 50% MGO to be able to use this fuel on the test bed.

Agarwal and Chaudhury [10] tested Karanja biodiesel and investigated spray tip penetration, spray cone angle and spray area. The higher viscosity of biodiesel resulted in loss of flow efficiency and reduction in injection velocity, still spray penetration was marginally higher, cone angle was lower and liquid length higher for biodiesel due to poor atomization, higher boiling temperature and the heat of vaporization. Galle et al. [11] investigated the influence of different types of biodiesel on the injection and atomization processes. They observed slightly longer spray penetration for unprocessed bio oils compared to biodiesel and petroleum diesel. Similar cone angles were observed for all fuels. Zhang et al. [12] looked at soot formation and utilized the two-color method to confirm that biodiesel is producing less soot.

In terms of biodiesel from fish oil used in marine application there is a lack of knowledge regarding the spray formation in sense of spray angle, penetration length and lift-off length. Aesoey [13] and Ushakov et al. [3] showed that fish oil has a similar potential to reduce soot formation as biodiesel produced from other feedstocks. They also showed that it can be applied as fuel for marine engines, but no optical investigation has been conducted so far.

Experimental setup

The test facility used in this study is a so called Constant Volume Pre-Combustion Cell (CVPC) and it is a basic investigation tool to separate the combustion process from all other engine influences and to simulate similar ambient gas conditions as those of an internal combustion engine due to compression [14].

The pressure and temperature conditions in the test cell is obtained with a chemical heating process described in the pioneering study of Oren et al. [15] and others [16] [17]. The cylindrical volume in the CVPC has a diameter of 250 mm and a volume of 5 dm^3. Two quartz glass windows with a diameter of 150 mm provide optical access to the combustion chamber from two sides. With this experimental setup, the CVPC is able to sustain a maximum vessel pressure of 100 bar due to stress limitations of the quartz glasses.

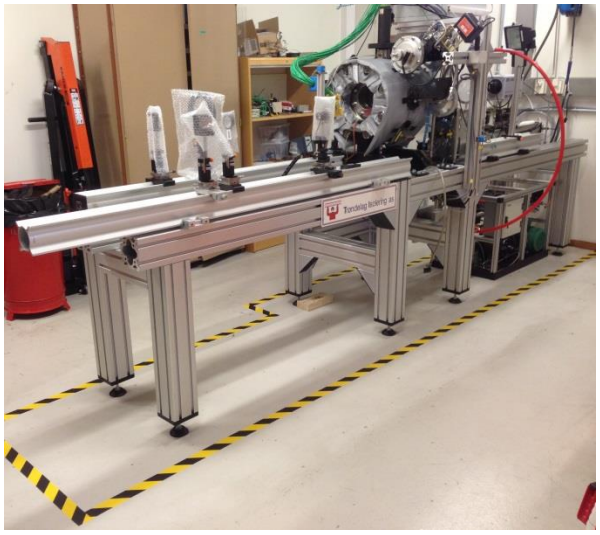

Figure 1. CVPC lab at Marintek/NTNU

For the pre-combustion heating process, the CVPC is filled with a combustible gas mixture of CO, N_2 and O_2, which is ignited before the injection starts. The gas is mixed outside of the CVPC in a specially designed gas mixer. After mixing, the gas is fed into the combustion chamber at a specific pressure and temperature.

This so called Pre-Combustion (PC) heats up the charge in the CVPC and supports a definite pressure and temperature for the main injection and combustion of the diesel fuel. The PC is initiated by a spark plug. After PC is completed, the combusted gas content has an oxygen level of 21 vol% and is an air simulated oxidizer for the main combustion when injection of fuel starts. The combusted gas was analyzed with a Horiba PG250 and the gas mixing process was optimized in order to get a residual O_2 content of about 21 vol%.

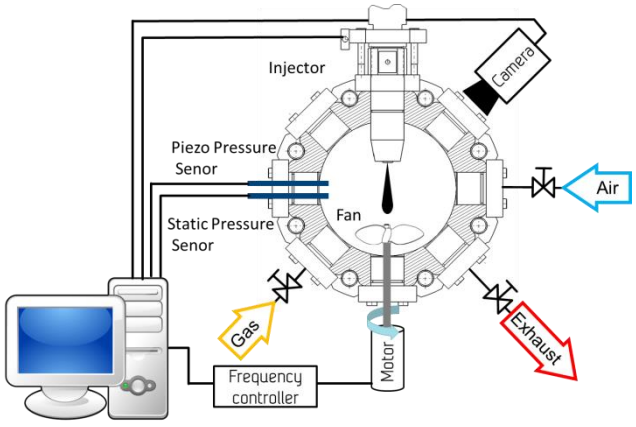

Figure 2. Schematic flow plan CVPC

Figure 2 presents the schematic function of the CVPC. The PC premixed gas is fed and regulated by a gas inlet valve and mixed with a fan to get more homogenous conditions. After PC and injection of the fuel the exhaust gas is flushed out with air (opening the air inlet valve) through the exhaust valve. The control of the experimental procedure and the data acquisition is done by an in-house generated system in LabView.

The injector is connected to a common rail system with a high pressure pump able, to supply a maximum pressure of 1800 bar, and a fuel temperature conditioning system. The system is designed for all kinds of biofuels and this means all pipes, hoses, valves, etc. are resistant to fuels with a high corrosive tendencies. In Table 1, the important injector parameters are summarized.

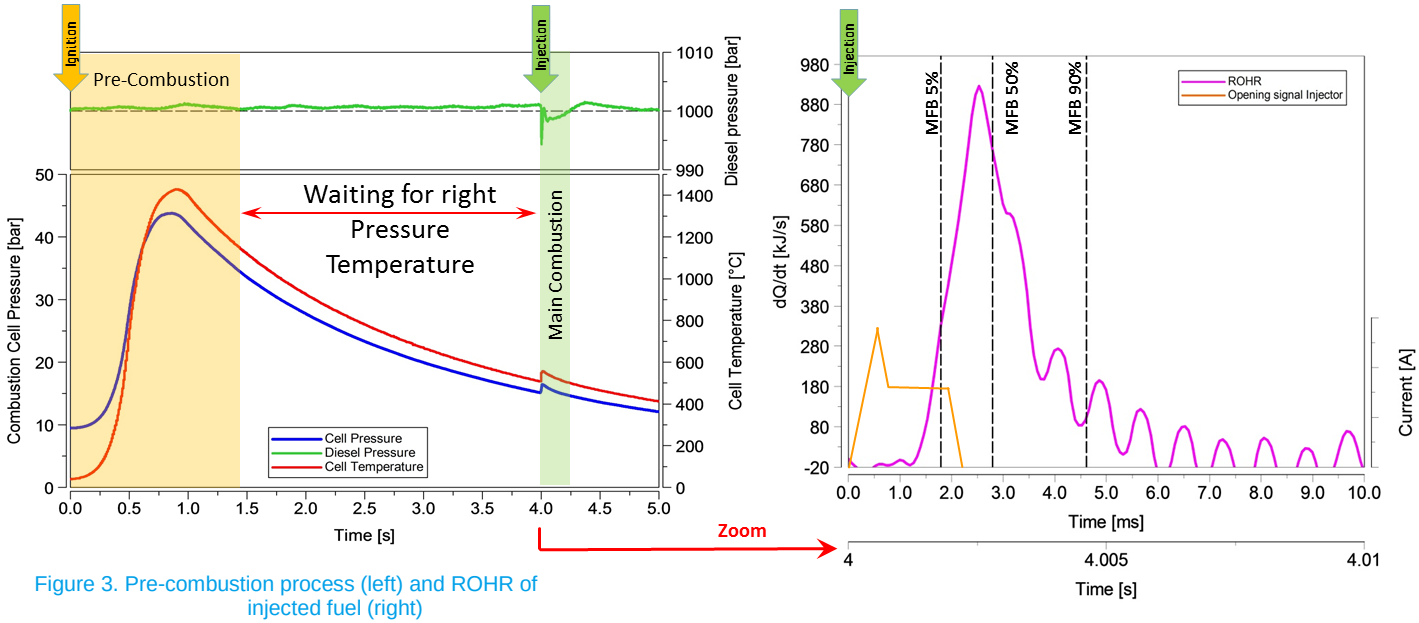

Figure 3. Pre-combustion process (left) and ROHR of injected fuel (right)

Figure 3 (left side) shows the experimental procedure with the pre-combustion (PC) and a waiting period followed by the injection of the fuel at the wanted temperature. During the PC, temperature (red line) and pressure (blue line) in the chamber increase. Due to the heat losses to the wall, temperature and pressure decrease until the fuel is injected. The burning fuel again increases the pressure and the temperature, but much less than during PC. The pressure traces are used to calculate rate of heat release (ROHR) of the burning fuel (Figure 3 right side). For the ROHR a new time line introduced where zero is counted when the electrical opening signal is sent to the injector.

For the injection system, a L'Orange solenoid medium speed engine injector was used with an single-hole nozzle. The injector was special produced for these experiments. A single-hole injector makes the spray investigation easier because the spray can be centered in the optical access and there is no interference of other sprays.

Table 1: Injector nozzle parameters

Description	*Value*	*Units*
Single hole injector outlet diameter	0.38	mm
Nozzle K factor	0.7	-
Q100	751	ml/min
Spray full included angle	0	deg

Table 2: CVPC Dimension

Description	*Value*	*Units*
Exterior diameter	420x420x400	mm
Interior diameter	D250xL100 (cylinder)	mm
Cell volume	5	dm^3
Max. gas temp	1800	K
Number of optical accesses	2	-
Quartz Glass diameter	150	mm

Table 3: Common Rail System

Description	*Value*	**Units**
Maximal pump pressure	1800	bar
Maximal piping pressure	2500	bar
Fuel temperature condition	288 - 333	K
Fuel resistance	All kind of bio fuels	-

CVPC Test conditions

For all experiments, the cell temperature was set to 873 K with a constant gas density of 12.2 kg/m^3.The oxygen level of the gas was 21 vol% to simulate air. It was very important to keep the cell gas properties during the test as constant as possible. Small variation in the gas temperature would lead to different combustion behavior of the fuel (like ignition delay, soot radiation and spray formation). The gas density in the cell could, during the time of the experiments, not exceed 12.2 kg/m^3, because the peak pressure of the pre-combustion was limited to 100bar. There are now further plans to redesign the cell for higher density in future studies.

The injection pressure was chosen to 800 bar, 1000 bar and 1400 bar to investigate the spray and combustion characteristic at different pressure levels. During the experiments the injected energy for all fuels was held constant to 3011 J by adjusting injection duration (see section fuel properties).

Table 4: Injection and spray combustion condition

Description	*Value*	Units
Cell density	12.2	Kg/m^3
O_2 concentration after pre-combustion	21	vol%
Gas temperature	873	K
Diesel rail pressure	800-1000-1400	bar

Image Processing

For the experiments two different optical methods on reactive sprays are used, Schlieren method to analyze the spray geometry and direct imaging to evaluate the soot intensity. With Schlieren, technique the first spatial derivative of the gas density in the chamber is detected, which makes this method useful to evaluate macroscopic spray scales [18].

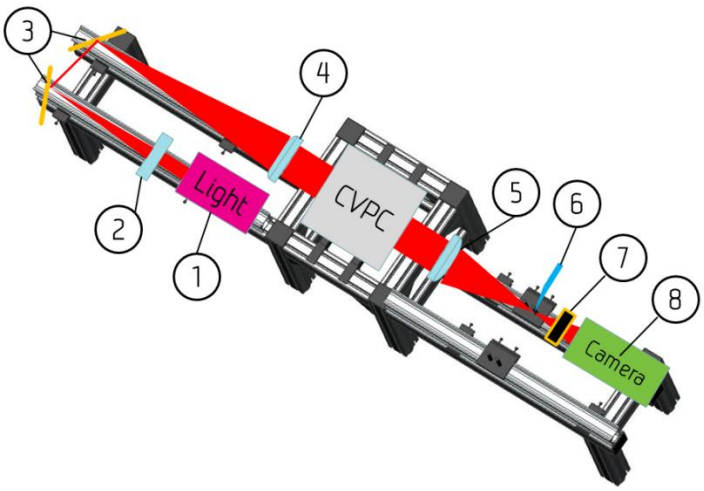

Figure 4: Optical setup

Eight injections were done at each injection pressure for all fuels, and the results were averaged to get a basis for statistical evaluation as well as to limit the risk of drawing conclusions based on faulty experiments.

In Figure 4 the schematic Schlieren setup is illustrated. A LED lamp (1) was used in combination with a condenser lens (2) to generate a dot shaped light source. With two mirrors (3), the light is leaded to the other optical rail. This rail was in line with the CVPC and the light beam was widened and parallelized in the first collimating lens (4) before entering the optical access. After the light beam has penetrated the CVPC, the light passes a second collimating lens (5) where the beam was again focused. A knife-edge (6) was positioned in the focal point of the second collimating lens. The knife-edge was oriented vertically to cut the focal point from the side to study density gradient in the spray direction. The CCD camera (8), Photron APX, is located behind the knife-edge and a KG1 colored glass band pass filter (7) (315 - 725 nm) was used.

In case of direct imaging, the first optical access (left side) of the CVPC was blocked, the optical equipment on the left side (position 1 until 4) and the knife-edge (6) was not used. The KG1 colored Glass band pass filter (315 - 725 nm) was in front of the camera. To analyze and compare the different soot emission levels of the different fuels the average background image is calculated and the cumulative intensity of the images was computed. To reduce the influence of the background noise, the intensity of the first picture with no combustion is subtracted from all the other pictures. The averaging of the broadband radiation (captured in digital intensity) of the image for every time step can be used for qualitative soot formation estimation, because more soot will introduce more broadband radiation and therefore higher intensity [19] [20] [21]. Figure 5 illustrates the position of the injector and the camera view. The single-hole spray develops in the injector axis and traveled from the top until to the lower part of the window.

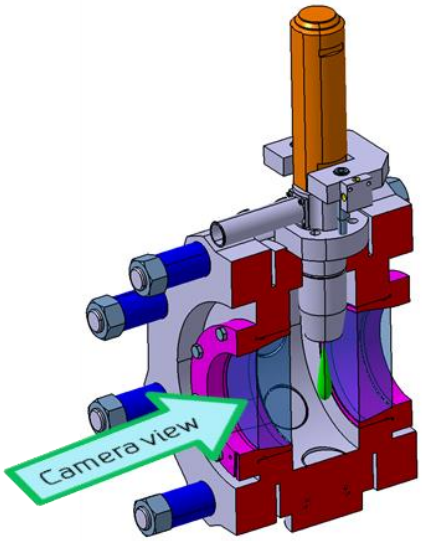

Figure 5. Camera and injector position

Figure 6 shows an example result of the two optical methods (Schlieren (a) and direct imaging (b)). A script in Matlab was written to convert the raw gray scale pictures captured from the high-speed camera to a dimensionless intensity picture. The

intensity classification was specified with the minimum and maximum intensity values after subtracting the background noise (Figure 6 right side).

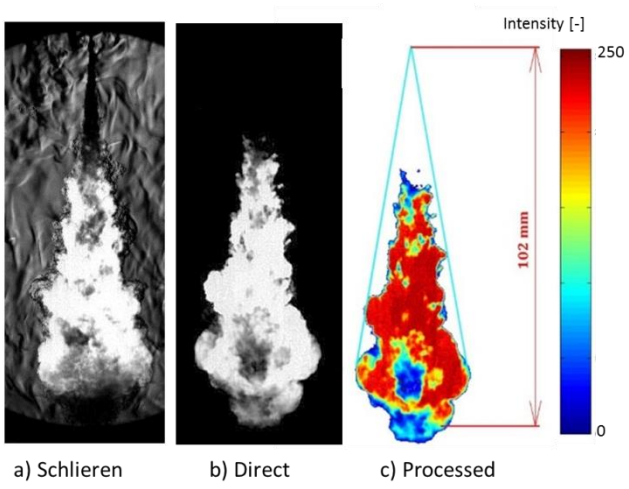

Figure 6. Intensity converted picture of spray combustion

Figure 7 demonstrates the picture average intensity history during a fuel combustion spray like in Figure 6. For all pictures during the combustion sequence, the averaged intensity value was calculated and plotted over the time scale. This diagram gives information about the qualitative soot formation during the combustion and quantifies the start and end of combustion.

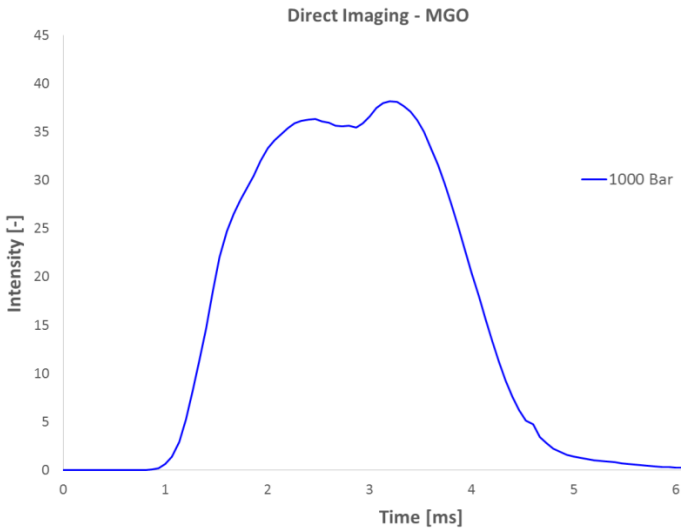

Figure 7. Averaged picture intensity history

Diffusion flame parameters like penetration length, cone angle and lift-off length (LOL) plays an important role in the mixing and combustion process. These parameters can be extracted from the captured images using an in-house developed analysis program (code in Matlab).
The first step is to establish a scale between pixels and a distance (mm) to measure the penetration length and LOL. This was done (before starting the experiments and after adjusted the camera) with an implemented ruler in the CVPC approximately where the spray appeared. Comparing the length of the ruler with number of pixels leads to the scaling factor. To measure the penetration length and the LOL, the picture was cut from the spray area of interest. With a constant threshold (value 125 RGB) the area of spray and background was subtracted. This process is also called masking procedure of the spray edges and turns the picture from gray scale into a black and white picture. After the picture is turned into black and white, the penetration length, cone angle and LOL can be found by searching minimum and maximum values along the nozzle injector axes.

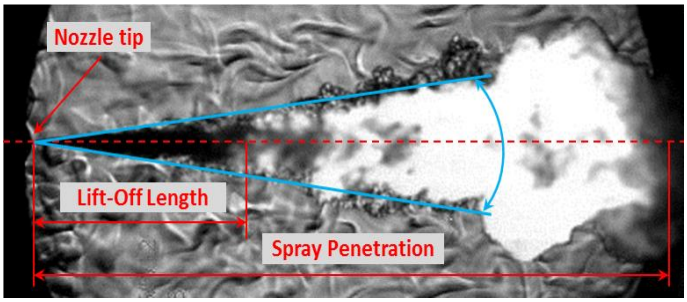

Figure 8. Definition spray penetration, spray cone angle and Lift-Off length

Figure 6 (right side) shows the masked picture cut in the way to investigate the spray of interest. Figure 8 illustrate the measured penetration length and LOL.
For all different fuels, the optical adjustments like shutter timing pictures per second and aperture were kept constant to be able to compare the results directly. The used components and the camera settings are listed in Table 5.

Table 5: Optical equipment and camera settings

Setting/Part	
Lens	Nikon 50mm
Filter	KG1 315-725 nm
Mirror	Gold Mirror 2"
Camera	Photron APX
Ligth source	Compact with LED Lights
Frame Rate	15000 pic/s
Resolution	256x496 pixles
Aperture	5.6 [-]
Shutter	1/500.000 seconds

Fuel properties

In general, the biomass for production of the biofuel is derived from a huge variety of raw materials; among them are municipal wastes, industrial effluents, agricultural products, algae, wood chips, animal and fish wastes and so on.

Norway has a historically developed fish industry, which could provide its own unique way in alternative fuels. The last decade, Norway has had a total annual fish production of approximately 3,5 million ton. More than 20% of this amount is considered waste and could have be partly utilized for fuel processing [22]. The main parts of fish that are convenient for oil extraction are: head, trimmings, viscera and skin.

Table 6 Fatty Acid Composition of the tested Fish oils

Fatty Acid	*Chemical Structure A:B**	*Weight %* CFO	FAEE
Myristic	C14:0	2.75	18.97
Palmitic	C16:0	8.84	31.30
Palmitoleic	C16:1	4.34	23.46
Hexadecatetranoic	C16:4	-	4.50
Stearic	C18:0	2.5	2.30
Oleic	C18:1	42.03	9.07
Linoleic	C18:2	13.09	0.95
Linolenic	C18:3	4.93	1.11
Stearidonic	C18:4	0.84	2.40
Arachidic	C20:0	0.33	-
Eicosenoic	C20:1	4.79	-
Eicosadienoic	C20:2	1.43	-
Eicosatetraenoic	C20:4	1.56	0.43
Eicosanoic	C20:5	2.73	5.05
Behenic	C22:0	0.38	-
Erucic	C22:1	3.62	-
Docosapentaenoic	C22:5	1.46	-
Docosahexaenoic	C22:6	3.99	0.47
Tetracosenoic	C24:1	0.39	-
Weight% Chain Length Range C14 - C16		15.9	78.2
Weight% Chain Length Range C18 - C20		74.2	21.3
Weight% Chain Length Range C22 - C24		9.90	0.50
Weight% Saturated Fatty Acids		14.8	52.6
Weight% Mono Unsaturated Fatty Acids		55.2	32.5
Weight% Poly Unsaturated Fatty Acids		30.0	14.9

**A – Carbon Chain Length, B – Number of Double Bonds*

To better analyze the results from this study, it is important to know the chemical composition and the different characteristics of the fuels. To obtain this information, the different fuels were sent to analysis. The fuel characteristics were established be Petrotest AS and Independent Inspection Services AB, whilst the chemical composition was established in the laboratory at Marine Ingredients AS. The chemical compositions of the fuels are presented in Table 6 and Table 7. The most obvious difference in fatty acid composition lies in that FAEE mainly consists of fatty acids with short carbon chain lengths, whilst CFO has a more spread distribution with Oleic and Linoleic as main components.

Table 7: Fuel composition (C-H-O-S)

	MGO	FAEE	CFO
Weight% Carbon	86.32	75.58	76.87
Weight% Hydrogen	13.63	11.98	11.9
Weight% Oxygen	0	12.44	11.23
Weight% Sulphur	0.05	0	0

The interesting value in Table 7 is the bounded fuel oxygen of the fish oil, which provides soot suppression during the combustion. The negative effect of the bounded oxygen is the decrease of the lower heat value. In the present experiments, the injected fuel energy was held constant and the injection opening timing was regulated to compensate for differences in LHV.

Table 8: FAEE and blends compared to MGO

	MGO	FAEE	50/50% MGO - FAEE	93/7% MGO - FAEE
Density [kg/m3]	849	874.8	862.5	852.7
Viscosity [mm2/s]	3.16	3.84	3.55	3.37
Cetane Index	48	56	49.9	49,4
Acid Number [mg KOH/g]	-	0.1	0.1	0.1
LHV [MJ/kg]	42.74	37.54	-	-
Oxidation Stability [Hours]	-	>0.5	-	-

Comparing the pure FAEE with MGO (Table 8) shows quite a different in density, viscosity and lower heat value (LHV). As described above the lower LHV is related to the bounded oxygen and in sense of energy density it is definitely a disadvantage. The higher density reduces this effect, because per injected volume more mass of FAEE fuel is injected. But still to be able to inject the same energy as for MGO the injector opening duration had to be increased by approximately 10%. This can be seen in Table 10. An important parameter for the spray characteristics is the fuel viscosity. Regarding to the spray theory [23] [20] it will influence the penetration length and the cone angle (see more in section spray analyze). For the blend of FAEE with MGO the properties are in between of pure fuels.

CFO (Table 9) shows large difference in properties comparing to MGO. Quite different is the viscosity from MGO and is approx. ten times higher. This was the reason why this fuel was not tested pure. The LHV of CFO is similar to the FAEE, but the density is higher, means the injected volume was slightly less than for FAEE.

Table 9: CFO and blends compared to MGO

	MGO	CFO	50/50% MGO - CFO	93/7% MGO - CFO
Density [kg/m3]	849	921,9	890.7	857.5
Viscosity [mm2/s]	3.16	31,5	10.5	3.91
Cetane Index	-	36,4	44.3	50.7
Acid Number [mg KOH/g]	-	>0.1	>0.1	1
LHV [MJ/kg]	42.74	37.19	-	-
Oxidation Stability [Hours]	-	3.8	-	-

Determination of the cetane number is a very expensive and tedious procedure and for this reason, there has been a developed correlation to predict cetane number based on other

fuel properties [20]. Cetane index is one of these correlations and in the standardized test method ASTM D4737. This method to predict the cetane number for biodiesel has however been criticized by several authors and some uncertainty in the test results have to be expected. Graboski and McCormick [24] claim that the cetane index is dependent upon the fuels aromaticity, and that it lacks significance for biodiesel since biodiesel has no aromatics. This can also be seen by looking at the cetane index in table 8. The blended fuels show very little difference in cetane index even though there are big differences for the pure fuels, and these values may be inaccurate.

Another important fuel property is the oxidation stability and refers to the chemical resistance to react with oxygen. This is of great importance when the fuel is subject to long-term storing. For biodiesel, the oxidation stability is the biggest issue and it has been reported to be the cause of increasing acid value, increasing viscosity and the formation of insoluble sediments, which compromise engine performance and the fuel system reliability [25]. Oxidation stability is not directly related to the combustion performance itself but is important for the fuel storage.

The result of the oxidation stability tests shows that the biofuels are unstable. This was expected, but the magnitude of instability was unexpected and it is the author's assumption, that the tested biofuels in this study are not prepared according to any fuel standard because their current main application is not as fuel. The FAEE has an oxidation stability of less than half an hour and a color change was observed during the FAEE testing in the CVCC. During the course of a couple of days, the FAEE turned from transparent to light yellow indicating a chemical change. Means to be able to use fish oil as alternative fuel antioxidants have to be added to have control of long time storing (bunkering).

Fish oil extraction and testing conditions

In this study two fish oil based biofuels and their blends, with different depth of processing, are tested. One Fatty Acid Ethyl Ester (FAEE) and one Crude Fish oil (CFO). Both are extracted from fish industry waste. The FAEE has been mechanically treated (purified) and in the second step esterified (transesterification reaction) to get a distillate fuel. The transesterification process is done in a chemical reactor where fish oil and alcohol in combination with a catalyst is reacted. A byproduct of this process is glycerol. In case of the CFO production, the process is simplified with a mechanical treatment, like degumming, purification and drying. A chemical process like esterification is not done and therefore CFO is different in sense of color, viscosity and odor. FAEE is transparent liquid with viscosity similar to diesel fuel, while CFO is viscous dark brown liquid with specific fish smell.

Due to higher viscosity of CFO and in order to avoid possible clogging of the fuel filters during test, the CFO was not tested pure. Instead, a blend of 50%MGO and 50%FAEE was decided to be tested because it was used successfully in previous studies [3]. As it was mentioned above, MGO has been chosen as a reference fuel to form a baseline in the current study. This fuel is characterized by low Sulfur content (0.05%) and is almost free from ash and asphaltenes. Detailed information regarding the studied fuels is collected in Table 6.

The same biofuels were tested in diesel engines prior to this investigation [13] and significantly lower PM emission values were obtained with the FAEE blends. Therefore, the objective of this particular study is to look closer into the soot formation in the CVPC.

Table 10: Injector opening timing and injected volume for constant energy

Rail pressure [bar]	MGO	FAEE	50/50% MGO-FAEE	93/7% MGO-FAEE	50/50% MGO-CFO	93/7% MGO-CFO	
800	760	880	820	770	660	750	[µs]
1000	560	620	590	560	530	560	
1400	400	430	420	400	390	400	
800	82.7	91.59	87.15	83.6	84.65	83.8	[mm3]
1000	82.9	91.27	87.1	83.6	84.41	83.8	
1400	82.4	91.39	86.9	83.6	84.99	83.8	

The 93%/7% blends were just tested for 1000 bar with direct imaging method, because the difference in the spray characteristic were very small. Table 10 is listing the different injector opening timing and injected volume for all fuels. The 93%/7% blend was chosen due to that this currently is the maximum biodiesel blend allowed by the EN590 diesel specification.

As discussed above, to inject the same amount of energy for the different fuels (taking into account the different LHV), the opening duration of the injector had to be adjusted. Since the single hole injector was made just for research purpose, no injector delivery curve was available. Therefore the delivery curves were measured separately for pure MGO, FAEE and 50%/50% blends. The delivery tests for the 93%/7% blends were not performed due to the negligible difference from MGO. The different viscosity of the fuel had an influence on the deliver curves, especially for CFO. To inject the same amount of energy with the 50%MGO/50%CFO, the injected volume had to be increased by approximately 2 mm^3 (see Table 10). What is Interesting to see is that in this case the injector opening timing had to be reduced from 560 µs to 530µs, and the reason for this is the higher viscosity of the fuel and therefore the slower closing operation of the injector needle.

Results and discussion

Combustion intensity-based on broadband radiation

The result of the direct imaging was an intensity history of the combustion process for the compared fuels as show in Figure 9. As described above the fuels are tested with three different injection pressures. Figure 9 shows the intensity history for three different injection pressures, where the time scale starts when the electrical opening signal is sent to the injector. All the results from the analysis of spray characteristic are adjusted for ignition delay. This means that all fuels are shifted to an averaged ignition delay. This makes the fuels individual spray development easier to compare and the trends more clear. As expected, the change of injection pressure had an influence on the intensity level and on the combustion duration. Higher injection pressure improves the fuel spray atomization process and results in smaller fuel droplets. Smaller droplets reduce the soot formation due to the enhanced mixing process causing

more complete combustion [26]. The trend of decreasing soot intensity with increasing injection pressure was observed for all fuels. MGO showed highest soot formation and FAEE the lowest with the blends in between for all injection pressures.

Due to the same injected energy for all three injection pressures the injection time will be shorter for higher pressures. When the combustion starts, the intensity is sharply rising before it levels out. In this time period the spray was fully developed and traveled later out of the visible area (out of the quartz glass window). This can be noticed from a slightly decrease of intensity in the diagram. When the injector needle was closing the spray momentum is decreasing and therefore the lift of lengths decrease. This means the fuel started to burn almost to the nozzle tip and this makes again a bigger slop on intensity increase. After injector needle was closed the spray decomposes and travels out of the window.

For 800 bar and 1000 bar the increase of intensity for FAEE started slower as for the other fuels. It seems like that FAEE had a large ignition delay. As discussed above, the ignition delay for the different fuel is canceled out. This means that FAEE has in the start a quite low intensity level and therefore lower soot level. This can be also seen from the spray pictures in Figure 20. For 1400 bar the different in the start intensity is very similar. The end of combustion for FAEE gives a wrong impression, because it looks like that there was a strong decrease of intensity. Due to the slightly longer penetration length of FAEE compare to the other fuels the spray is earlier out of the quartz window and produced less intensity. However, the end of combustion is not really precise to analyze because some of the fuel sprays were out of the window and radiation appeared from not fully atomized diesel droplets at the end of injection. This is also called after dipping.

If the injector needle closes, there is still fuel in the sac volume, but the high pressure is not active at the nozzle seat [27] and the atomization process is therefore not working correctly and the result is fuel droplets leaving the nozzle hole. This can be also noticed further in the ROHR analyze.

When MGO was blended into the fish oils the intensity level increase. For the 93%/7% blends, the differences in intensity compared to MGO was very small and the difference is within the range of the standard deviation of the measurements.

The 50%/50% blend of MGO and CFO had slightly higher intensity as 50% MGO/50% FAEE for 800 bar and 1000 bar. For 1400 bar the two fuels behave very similar and this effect can be related to the better atomization effect of the spray at higher pressure.

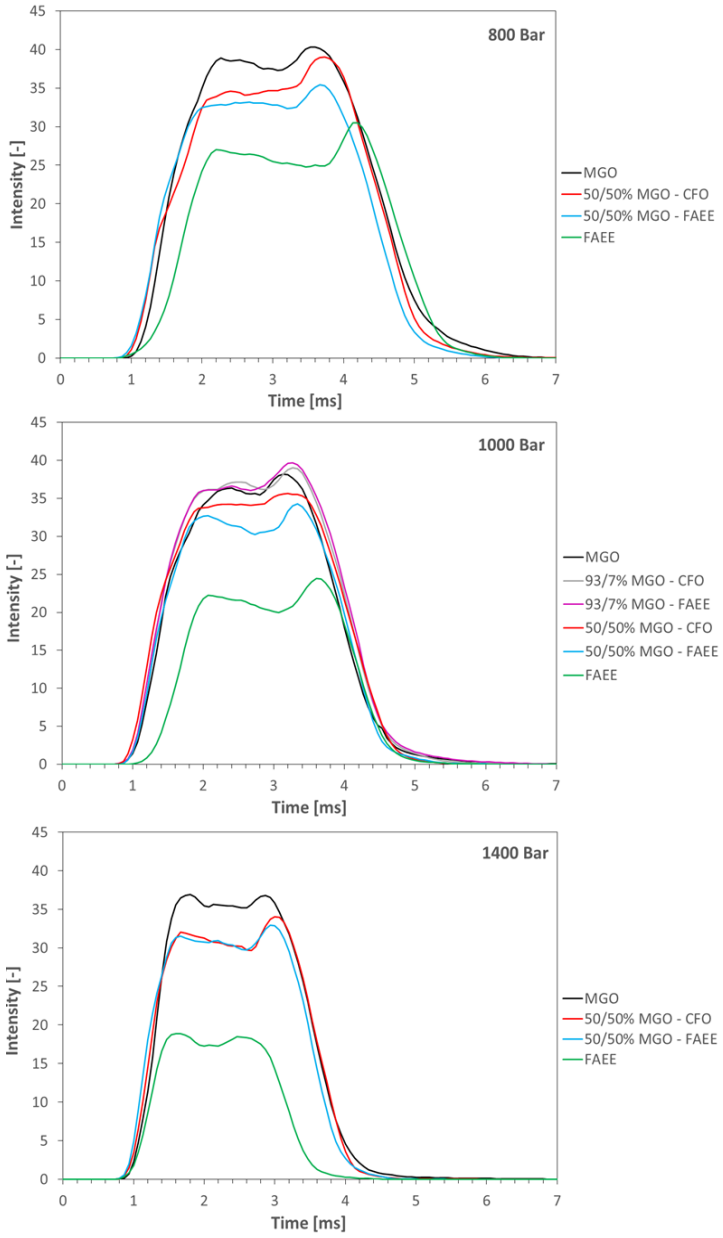

Figure 9. Intensity history during the combustion for MGO, FAEE, 50%MGO/50%FAEE and 50%MGO/50%CFO

A possible explanation for the higher soot formation from MGO compared to the fish oils are the aromatic and sulfur contents of MGO and the presence of fuel bound oxygen in both fish oils (see Table 6). Especially the fuel bound oxygen plays an important role for a more completed soot oxidation. This was also the conclusion in [28] [29] [3].

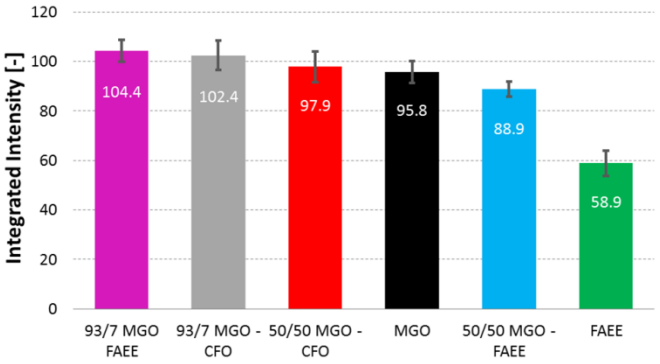

Figure 10. Integrated image intensity during combustion for all fuels and fuel blends, 1000 bar Injection pressure and approx. 3 kJ constant injected energy

Figure 10 represents the integrated intensity during the combustion (not included end of combustion) and corresponds to the area under the graph in Figure 9 for 1000 bar. As described above the 93%/7% blends had a slightly higher integrated intensity then MGO, but this difference was almost within the value of the standard deviation. Therefore it can be assumed that this blends had a similar soot behave as MGO.

The integrated intensity shows again the high potential on soot reduction of FAEE with the smallest value. This potential was reduced if MGO was blended in (see 50%MGO/50% FAEE).

In Figure 9 (pressure case 1000 bar) soot intensity history for the blend 50%MGO/50%CFO can give a wrong impression about the total soot intensity, because the fuel shows a lower intensity during the time period 1.4 ms up to 2.8 ms. During the start of combustion the intensity of the blend was higher than for MGO and therefore the integrated intensity in sum was also higher (see Figure 10)

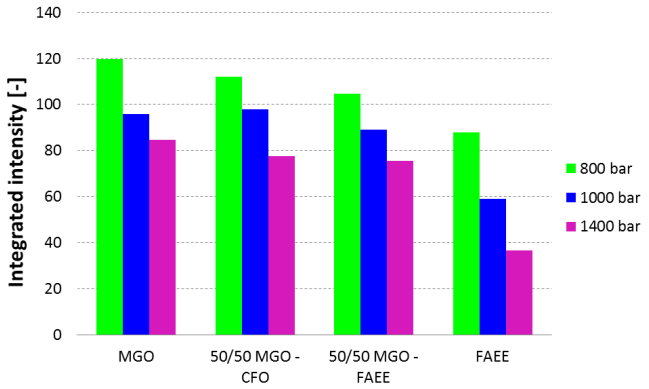

Figure 11. Integrated image intensity for all tested rail pressures and 3kJ injected energy

In Figure 11 the integrated intensity for 800 bar, 1000 bar and 1400 bar are shown and compared to each other. All fuels following the same trend of increasing rail pressure decrease the soot radiation intensity. Special FAEE shows the strongest influence on the rail pressure.

Spray analysis

The next section will discuss the spray characteristic for the different fuels. The different fuel properties like density, viscosity etc. have an impact of the spray formation and therefore of the combustion itself. It was observed in other references that fish oils with higher viscosity have longer penetration length and narrower spray cone angles [11] [10]. It was stated that higher fuel viscosity, increase the droplet size in the spray and leads to higher spray momentum. Higher momentum means higher penetration length and therefore also less impact between ambient gas and fuel spray (means narrower cone angle).

Spray penetration

In Figure 12 the penetration history during the combustion, captured using Schlieren method, is presented at 1000 bar injection pressure. For better comparison of the different fuels, the ignition delay was canceled out to make the combustion starts at the same time.

In the beginning of the combustion MGO and the blend 50%MGO/50%FAEE had a slightly longer penetration length than pure FAEE and 50%MGO/50%CFO. It could be assumed that MGO and the blend 50%MGO/50%FAEE had the same value due standard deviation (see Figure 13). The same applies to FAEE and 50%MGO/50%CFO. After the spray combustion is developed, FAEE and the blend 50%MGO/50%FAEE increased the penetration length and both reached first the end of the optical access. CFO had during the further combustion a shorter penetration length.

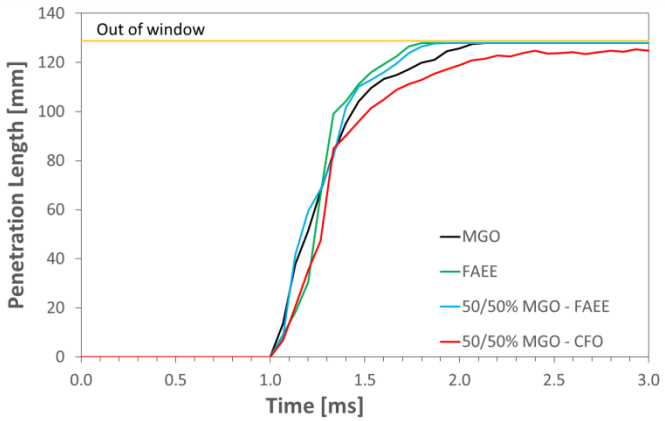

Figure 12. Penetration length during combustion at 1000 bar and 3 kJ constant injected energy

These results correspond with the spray theory since FAEE has a higher viscosity than MGO. The blend 50%MGO/50%CFO showed unexpected result since CFO has a much higher viscosity than MGO and FAEE. From these results no explanation is found and further investigation are necessary to investigate the shorter penetration length. It could be, due to the high level on viscosity for CFO, that the velocity losses in the nozzle were strong increased and therefore the penetration length reduced.

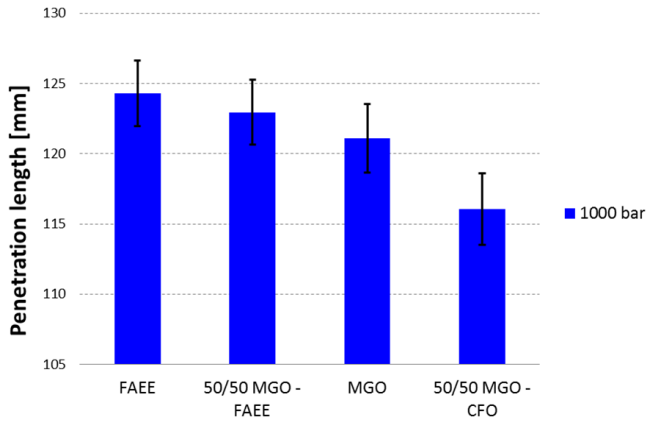

Figure 13: Averaged penetration length for developed spray at 1000 bar

Figure 13 presents the averaged penetration length during the combustion for 1000 bar. Averaged penetration means in the time window between 1.3 ms until 2. Here can be assumed the injector needle was full open and the spray starts further development. This chart bar helps to illustrated and high light the difference in the penetration for the different fuels. As described above FAEE recorded the longest penetration and in this case the blend 50%MGO/50%CFO the lowest.

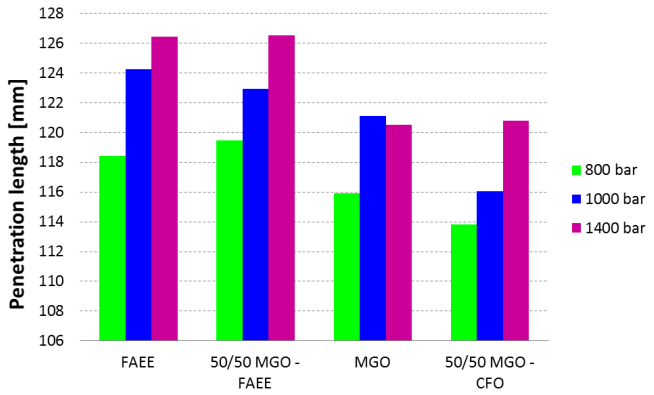

Figure 14: Averaged penetration length for developed spray at 800 bar, 1000 bar and 1400 bar

When the injection pressure was increased all fuels showed in general a longer penetration length and this was according to the higher spray momentum (spray theory). For higher pressure the blend 50%MGO/50%CFO overtake MGO and corresponds better with the spray theory. FAEE and 50%MGO/50%FAEE had for his pressure case similar result.

For a decrease of the injection pressure the penetration trend was similar to the 1000 bar pressure case, excepted from the blend 50%MGO/50%FAEE. This blend recorded the highest penetration length.

Spray Lift-Off Length

As discussed in the image processing section, the Lift-Off Length (LOL) is measured from the nozzle tip until the first soot radiation is captured. Normally the LOL is detected with OH radical equipment. However, for this project no optical OH radical dedication tool was available and therefore the soot radiation was taken for indication.

At start of soot intensity the LOL are similar for all fuels. FAEE and the 50%MGO/50%CFO showed a marginally shorter LOL than MGO and 50%MGO/50%FAEE blend. However, also here the differences of the fuels were quite small and it could be assumed that the LOL for each fuels are equal. During the combustion process the LOL for pure FAEE and fish oil blends starts to increase more than MGO. After approximately 3 ms the LOL starts first to decrease and later increase. The reason is that the injector needle starts to close and the spray momentum decrease. During this time the last part of the injected fuel with lower momentum burns closer to the nozzle tip. When the injector needle is closed, the spray travels away from the injector and the LOL increase again until the spray traveled out of the window.

The point where LOL starts to decrease and increase is small shifted between the fuels. The reason for this is the slightly different injection duration for all fuels due to the same injected energy.

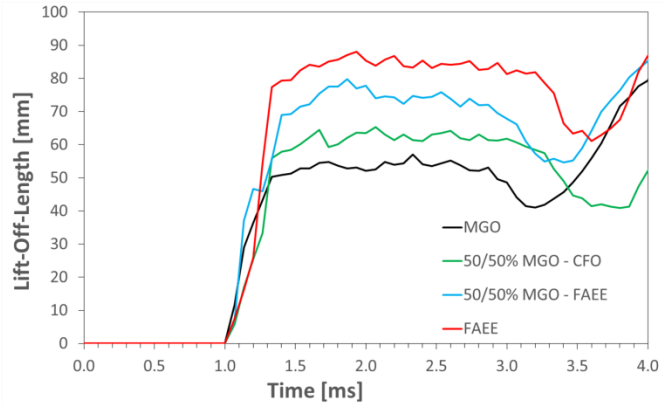

Figure 15. Lift-Off Length during combustion at 1000 bar and 3 kJ constant injected energy

In the time interval between 1.5 ms and 3 ms the LOL is more or less stable for all fuels (injector needle is full open) and the averaged LOL can be seen in Figure 16. The LOL can be seen as the area where fuel and oxygen is mixing until auto ignition conditions are reached [30]. A longer LOL indicates that the fuel spray needs longer time to mix with the ambient oxygen or because of lower auto ignition condition of the fuel (centane number), the spray has more time to mix with air and a lower equivalence ratio is resulting in the LOL area [30]. This further helps to suppress soot formation. Due to higher fuel viscosity and therefore expected bigger droplets in the fuel spray, the larger LOL can indicate that a not optimal fuel/air mixture process in this case. This could lead to disadvantages for fish oil regarding soot formation compared to MGO. Due to the bounded oxygen in fish oil the overall soot formation was still lower. For further investigation in this specific topic, the droplet size distribution for the different fuels have to be investigated and this will be done in future projects.

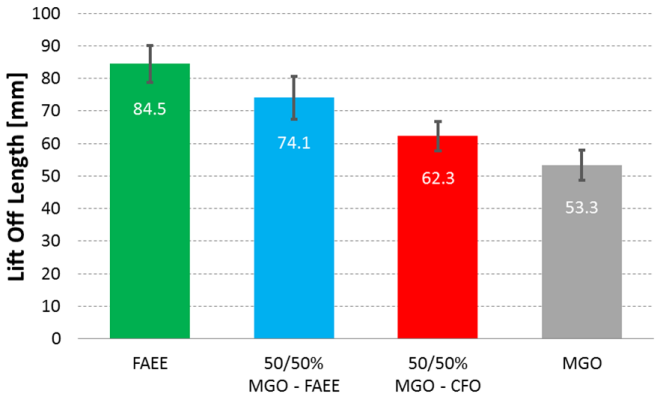

Figure 16: Averaged LOL between 1.5 ms and 3 ms

Figure 16 shows the described trend for the different fuels, with the highest values of LOL for FAEE and the lowest for MGO. A not expected result shoed the blend 50%MGO/50%CFO with a quite low value of LOL. Here the information of droplet size would help to explain this phenomenon.

Spray cone Angle

The spray cone angle results correspond with [23] and also the results from the penetration lengths. The spray theory states that longer penetration length corresponds to narrow angle and vice versa [23] [31]. MGO had from begin of combustion higher values and hold this higher values during the whole combustion process. The opposite results showed FAEE. Also here can be stated that the higher viscosity points to higher momentum in the fuel spray and therefore a narrower spray angle. Again the blend 50%MGO/50%CFO should present lower values for the cone angle and has to be investigated more in detail.

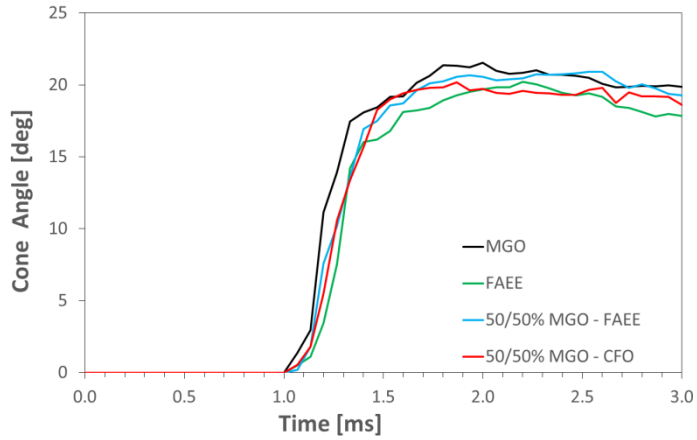

Figure 17: Spray cone angle during the combustion

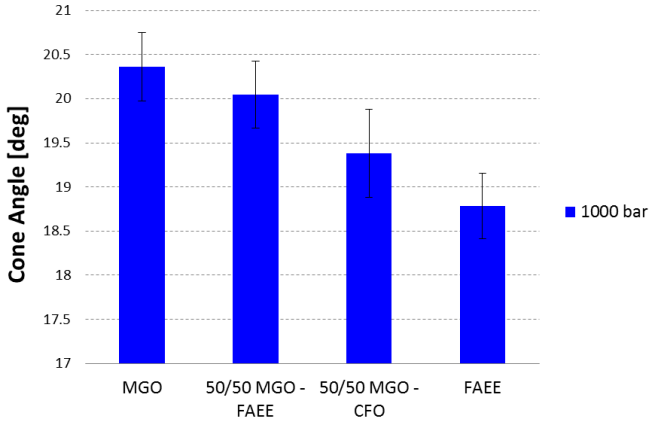

Figure 18: Averaged cone angle at 1000 bar for different fuels in the stabilized area

Figure 18 presents the averaged cone angle in the stabilized spray area (1.6 up to 2.8 ms) for the 1000 bar case. The bar chart diagram shows the described cone angle trend quite clear. MGO presented the highest value and FAEE the lowest, the fuel blends are in between.

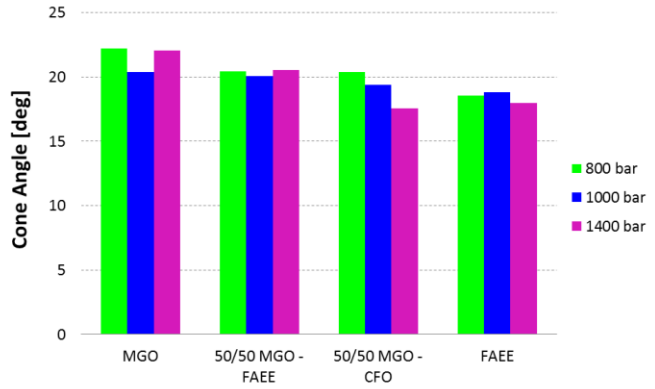

Figure 19: Averaged cone angle at 800 bar, 1000 bar, and 1400 bar for different fuels in the stabilized area

In Figure 19 the results of the cone angle for different injection pressure are plotted. The described trend was also visible for different rail pressures, means that MGO had all the time a larger cone angle and FAEE the smallest. For 800 bar the difference between the 50%/50% blends were very small and therefore they can be assumed as the same.

Combustion imaging of the tested fuels

Figure 20 shows one of the eight combustion series (raw pictures) of the different injected fuels for 1000 bar injection pressure. These images are a part of the data used for processing the spray image analysis given in Figure 12 up to Figure 19. The background of the Schlieren picture shows the density disturbance in the cell due to the pre-combustion process. As described in the imaging processing section, the Schlieren method is able to visualize gas density gradients. A stronger density gradient will be appearing as a dark area in the picture. The darkest area in the spray appeared from the nozzle tip until to the first location of the soot radiation. This area includes the liquid spray core (primary break-up) plus the air/fuel mixing zone. In these experiments the LOL represent the lengths of this core. The whole spray shape was slightly darker than the background. As discussed in the LOL section, FAEE showed a longer LOL and the fuel blends followed this trend. MGO represented a relatively short LOL compared to FAEE, which means it burned closer to the nozzle tip. This was also found in [10] and [11] for biodiesel and confirms that fish oil has similar spray properties as these fuels.

For the whole combustion of the pure FAEE, it can be seen there was less soot intensity compared to the other fuels and confirm the results from Figure 9 up to Figure 11. The blend of 50%MGO/50%FAEE showed more soot radiation in the middle section of the spray shape, but still a lower overall soot radiation than MGO. For the blend 50%MGO/50%CFO the local intensity seems stronger than for MGO, but also here the soot radiation appeared not in the full spray, so that the total intensity is less than for MGO.

The fuel-bound oxygen in the fish oil had a positive impact on soot formation because this oxygen increases the air–fuel equivalence ratio λ (lambda) and therefore reduces the soot formation. A negative impact of the bounded oxygen is the lower heating value for these fuels and it may further effect increasing NOx formation due to locally higher temperatures [4]. It would be interesting to investigate in more detail where the local soot radiation for the different sprays appears and how the NOx emission changes. Apparently there is a significant difference in where the soot radiation is located and at which magnitude. This will be investigated in further work to get a clear picture of the potential for emission reduction.

The soot radiation starts for all fuels in the middle section of the spray and expand through during the combustion, until the diffusive spray is established. All fuels showed less intensity on the tip of the spray.

It is also interesting to see the differences in spray shapes. When comparing the extreme examples MGO with the 50%/50% blend of MGO and CFO, it can be noted that the blend has an outgrowth on the left and right side at the lower third part of the spray. On the contrary, MGO has a clearer border between spray and surroundings. The other fuels (FAEE and 50%MGO/50%FAEE), presents a variation in between the extreme examples.

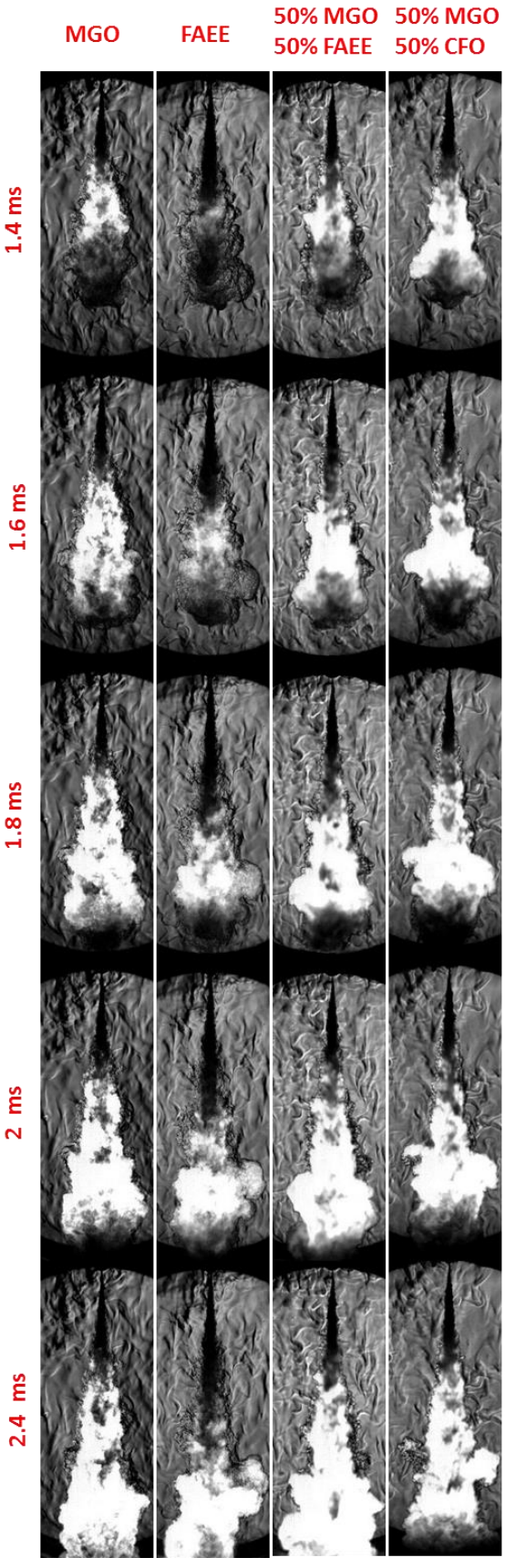

Figure 20. Image of the combustion process of the tested fuels from Schlieren imaging for 1000 bar

In general pure fish oil and the blends showed a larger spray tip and narrow spray angle (tail), this can be clear obtained from the pictures. For the section spray analyze, the spray angle was measured with not including the disturbance of the spray head.

At 1.4 ms the start of soot intensity for the different fuels can be seen. It should also be noted that in general the ignition delay between the fuels were not significant (see also the section thermodynamic analysis), but still at 1.4 ms the soot radiation of blend 50%MGO/50%CFO was more developed as for the other blends. At 2.4 ms the spray is stabilized and some of the spray tip is already out of the optical access.

Thermodynamic analysis

In this section the thermodynamic analysis from the pressure trace will be shown, in sense of rate of heat release (ROHR) and mass fraction burned (MFB). For this purpose a piezo electrical sensor was used (Kistler 6045A). To monitor statistical variations, every experiment was repeated 16 times and the averaged results are presented. Due to the large volume of the CVPC compare to the injected fuel mass, some inaccurateness regarding the duration of the ROHR and the soot intensity could be observed. The reasons for this is the big CVPC volume, end of combustion out of the visible area (spray out of the window) and random bigger droplets regarding the needle closing process.

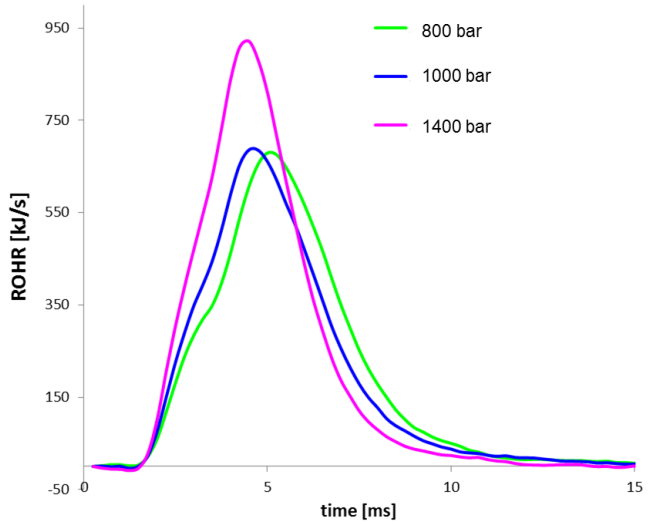

Figure 21: ROHR for different rail pressure; MGO

In the Section spray analyze it was observed that higher injection pressure decrease the soot intensity level and shortened the combustion duration. In Figure 21 the ROHR for three different injection pressures for the case study MGO are presented and the same effect is observed.

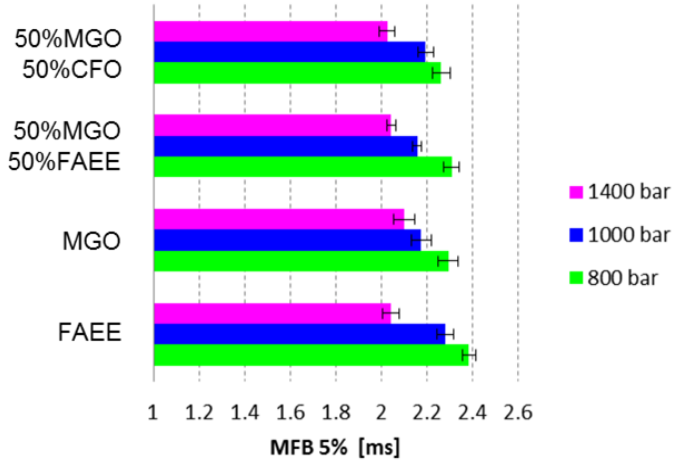

Figure 22: Comparing ignition delay for different rail pressures

For 1400 bar injection pressure the ROHR is more compact, had slightly shorter ignition delay (see also Figure 22) and the end of combustion was faster than for the lower injection pressures. The combustion started faster and a higher slope was recognized. In all injection pressure cases, the same amount of energy was injected. To release the same amount of heat energy for 1400 bar, the peak of the ROHR has to be higher (injected energy equal to the area under the ROHR). These results can be linked to the spray formation of the fuel. Higher injection pressure will improve the atomization process and suppress not only the soot production, but also the process time of combustion itself.

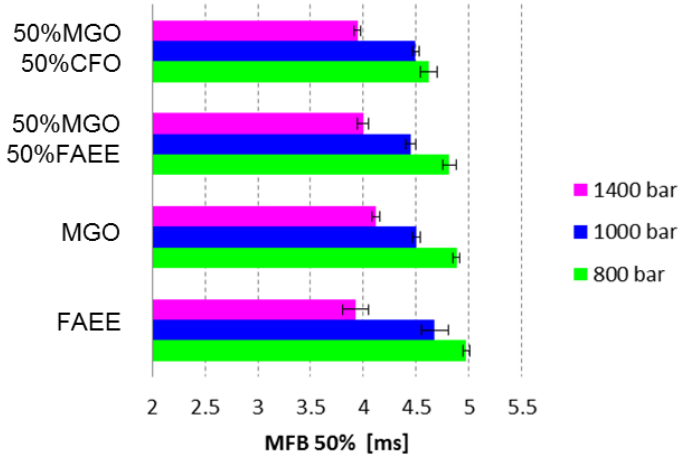

Figure 23: Influence of MFB 50% due to injection pressure

The opposite behavior was obtained from the 800 bar injection pressure. Start of combustion was longer delayed and the duration was the longest. Again, to release the same energy the peak value has to be lower, because the combustion duration was increased. The 1000 bar rail pressure showed the same trend and is between the 1400 bar and 800 bar case. In Figure 22 and Figure 23 the influence of MFB 5% (ignition delay) and MFB 50% due to the injection pressure variation for different fuels are summarized. The described trend could be

seen for all fuels where FAEE shows the biggest variation for variable injection pressure. The differences in MFB 50% between the fuels at the same injection pressure are noticeable, but still not very big in variation. FAEE presented mostly largest time value for the MFB50% (excepted for 1400 bar) and the blend 50%MGO/50%CFO the lowest values.

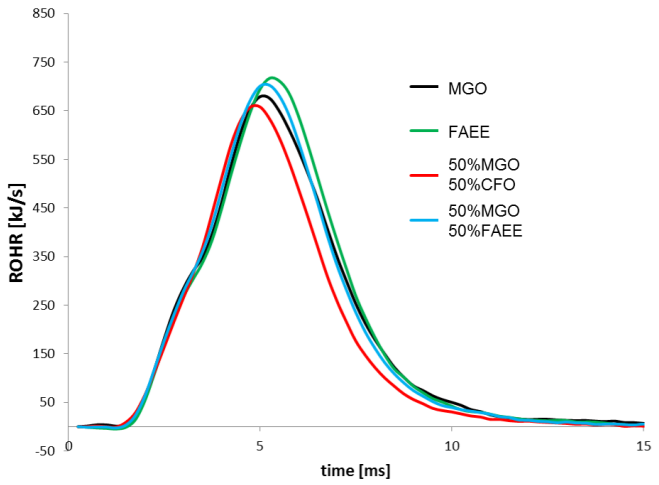

Figure 24: ROHR for 800 bar rail pressure

Comparing the ROHR of different fuels at 800 bar injection pressure leads to the diagram in Figure 24. The theoretical injected energy was also here tried to hold constant. It could be observed that the combustion process was different between the fuels, special in the end of combustion. The highest peak value was observed for FAEE and also the combustion duration was longer than for the other fuel. Compared to the blend 50%MGO/50%CFO gives the conclusion that although the injected energy was the same, the real combusted energy are quite different. This means the combustion efficiency from fuel to fuel was varying. Since the combustion start for all fuels were similar the distinction of sum burned fuel appeared more in the half of combustion and can be interpreted as not completed burned fuel. An explanation of this could be the bounded oxygen in the fuel, which increase slightly the combustion efficiency because more oxygen is available. This was also found in the studies from Zhang [4].

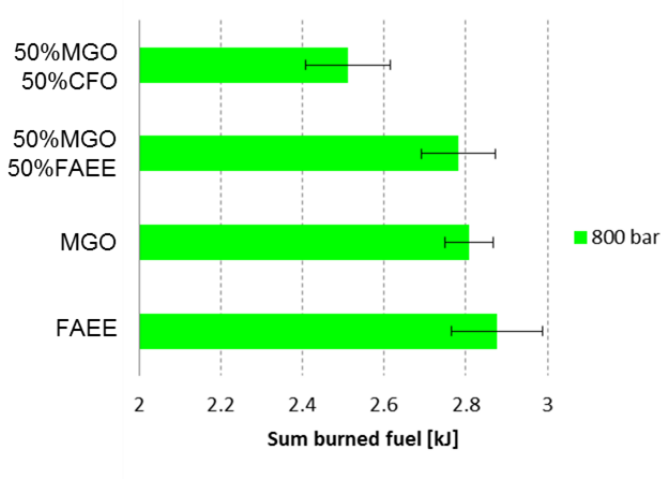

Figure 25: Total combusted fuel

The bar chart diagram in Figure 25 sums the explained ROHR diagram in Figure 24. The sum burned energy of the 50%MGO/50%CFO was in between MGO and FAEE if taking into account the standard deviation (error bar). The error bars in general also showed a higher variation for the fish oil and their blends means the cycle to cycle variation is higher for these fuels.

Summary/Conclusions

In this study, the spray combustion of two different fish oils (biofuels) and their different blends were optically and thermodynamically investigated and compared to MGO in a Constant Volume Pre-Combustion Cell (CVPC). One biofuel was an unprocessed crude fish oil (CFO) and the other was processed through transesterification of fish oil (FAEE). The crude fish oil could not be tested pure because of its high viscosity and was blended with MGO in a ratio of 50 vol% MGO to 50 vol% CFO. FAEE was blended with MGO in a ratio of 50/50% and 97/3%. In total six different fuels were tested.

It can be concluded that these fish oil fuels have a high potential to reduce soot emissions compared to MGO in marine engine applications. One reason for soot suppression could be the bounded oxygen, whereby FAEE has a higher potential on soot redaction than CFO. The level of soot formation was qualitatively measured with the image intensity of the spray combustion. This paper focused on the soot emission. Other emissions like HC and CO were not discussed.

Due to design limitation of the CVPC, the gas density in the cell was limited to 12.2 kg/m^3 and this could influence the spray shape of the injected fuel. For this reason, the results are not absolute values and have to be considered for relative comparison. For further work, the CVPC will be redesigned to facilitate higher gas densities.

The main findings of this paper are summarized in the following:

1. The image intensity history during the spray combustion showed lower soot intensity for the fish

oils compared to MGO. Pure FAEE showed the highest potential and depending on the injection pressure the soot suppression can be significant. It is assumed that the bounded oxygen has positive impact of the soot formation. CFO shows a lower soot reducing potential than FAEE, and it can be assumed that this is related to the higher viscosity and therefore a bigger droplet size in the fuel spray. Further investigation of droplet size distribution will give more information regarding this. The 93/7% blends shows no difference compare to MGO and the only benefit with these fish oil blends is that there is the presence of some renewable energy in the fuel. This also means that the combustion process is similar to MGO, which makes the use of this fuel easier with existing engine technology. It could be shown, that the injection pressure has similar influence for bio fuel as for MGO (regarding the spray and diesel combustion theory) on the soot intensity. The influence of injection pressure for FAEE was higher than for CFO and can be related again to the higher viscosity.

2. The chemical analysis revealed that the fish oils have a lower LHV than MGO, which is related to the bounded oxygen. Increasing the injection duration will compensate for this, but there are limitations. Special for higher BMEP and engines running on higher RPM (the limitations are given by the injector nozzle orifice). Regarding the oxidation stability, improvements has to be made if this fuel will be used in normal marine applications. This could be solved by adding additives.

3. The results of the fish oil combustion showed that penetration length and lift-off length were longer than for MGO. This means that fish oil has similar spray characteristic as biodiesels from other feedstocks. FAEE and its 50%/50% blend with MGO shows both longer penetration and lift-off compared to pure MGO. The same trend can be seen with increasing injector pressure. However, for the 50%/50% blend of MGO and CFO, this trend was not as clear. Especially for 800 bar and 1000 bar it had shorter penetration length than MGO. An explanation for this could be the almost three times high viscosity of this fuel, which could cause a lower spray momentum due to friction losses in the injector nozzle. In future work it is planned to measure fuel droplets distribution to better understand the break up regime of CFO.

4. The fish oils and their blends with MGO all showed longer LOL compared to MGO. If this had a positive or negative effect on the soot formation cannot be stated at this point. Normally a longer LOL can help to improve the fuel/air mixing process and therefore suppress soot formation. In case of fish oil the longer LOL is more related to bigger droplets and this means the fuel needs longer to mix and reach the auto ignitions conditions. This further indicates that with a better atomization process the potential of soot suppression for fish oil could be even higher. It should be stated here that normally LOL will be detected with OH chemiluminescence. This equipment was not available for these experiments and only the soot radiation could be used to measure the LOL. Therefore this value will be different than reported in other studies.

5. Due to the conclusion in point 3 and 4, it is obvious that a change in the injector geometry itself, like nozzle orifice, could help to use the full potential of fish oil. Means to achieve the same spray characteristics as for MGO, a hardware modification has to be done as well. Only changing the fuel in an engine application will not use the full benefits of these fuels.

6. From the Thermodynamic analysis it is shown that variation in the injection pressure had an impact on ignition delay and the MFB50%. This effect was observed for all fuels and fuel blends. Comparing the ROHR for one specific pressure case revealed a higher value for sum burned fuel for FAEE. This can be interpreted as the befit of bounded oxygen in the fuel. In the case of CFO the bounded oxygen cannot overcome the disadvantage of the higher viscosity and therefore different spray shape.

7. The injector itself did not show changes in injection characteristics after tests with fish oil. No malfunction of the mechanical function was noticed, but for a clear fuel/life time impact, these tests do not provide enough information to draw any conclusion.

8. To use fish oil as an alternative fuel in the maritime industry, further work has to be done. For Instance, oxidation stability is an important parameter for fuel storage and could be problematic with fish oil. In addition, the impact of fish oil on the mechanical parts of the fuel system has to be investigated as well.

References

[1] E. E. Agency, “Transport and environment:on the way to a new common transport policy,” European Environment Agency, Copenhagen, 2007.

[2] R. Edwards, “Well-to-wheels Analysis of Future Automotive Fuels and Powertrains in the European Context,” JRC Scientific and Technical Reports, Luxembourg, 2011.

[3] S. Ushakov, H. Valland and V. Æsøy, “Combustion and emissions characteristics of fish oil fuel in a heavy-duty diesel engine,” *Energy Conversion and Management,* pp. 228-238, 2013.

[4] J. Zhang, W. Jing, W. L. Roberts and T. Fang, "Soot temperature and KL factor for biodiesel and diesel spray combustion in a constant volume combustion chamber," *Applied Energy,* pp. 52-65, 2013.

[5] N. Mrad, E. G. Varuvel, M. Tazerout and F. Alour, "Effects of biofuel from fish oil industrial residue – Diesel blends in diesel engine," *Energy,* pp. 955-963, 2011.

[6] U. S. E. Protection, "A Comprehensive Analysis of Biodiesel Impacts on Exhaust Emissions," United States Environmental Protection Agency, 2002.

[7] M. S. Graboski and R. L. McCormick, "Combustion of fat and vegetable oil derived fuels in diesel engines," *Progress in Energy and Combustion Science,* pp. 125-164, 1998.

[8] D. K. Ramesha, R. K. Thimmannachar, R. Simhasan, M. Nagappa and P. M. Gowda, "A Study on Performance, Combustion and Emission Characteristics of Compression Ignition Engine Using Fish Oil Biodiesel Blends," *Journal of The Institution of Engineers (India): Series C,* pp. 195-201, 2012.

[9] D. K. Ramesha, P. M. Gowda, N. Manjunath and S. Rajiv, "Performance, Combustion and Emission Evaluation of Fish and Corn Oil as substitute fuel in Direct Injection C. I. Engine," *AMAE Int. J. on Production and Industrial Engineering, Vol. 4,* pp. 1-12, 2013.

[10] A. Agarwal and V. H. Chaudhury, "Spray characteristics of biodiesel/blends in a high pressure constant volume spray chamber," *Experimental Thermal and Fluid Science,* pp. 212-218, 2012.

[11] J. Galle, S. Defruyt, P. R. Rodriguez, Q. Denon, A. Verliefde and S. Verhelst, "Experimental investigation concerning the influence of fuel type and properties on the injection and atomization of liquid biofuels in an optical combustion chamber," *Biomass and Bioenergy,* pp. 215-228, 2013.

[12] C. S. Lee, S. W. Park and S. I. Kwon, "An experimental study on the atomization and combustion characteristics of," *Energy & Fuels 19 ,* p. 2201–2208, 2005.

[13] J. B. N. a. S. U. V. Aesoey, "Alternative marine fuels and the effect on combustion and emission characteristics," *CIMAC, no. 43,* pp. 1-12, 2013.

[14] R. Baert, P. Frijters, B. Somers, C. Luijten and W. Boer, "Design and operation of a high pressure, high temperature cell for hd diesel spray diagnostics," *SAE International,* p. No. 0649, 2009.

[15] D. Oren, B. Wahiduzzaman and S. Ferguson, "A diesel combustion bomb," *SAE International,* p. No. 841358, 1984.

[16] R. Fraser, R. Edwards and D. L. Siebers, "The autoignition of methane and natural gas in a simulated diesel environment," *SAE Iinternational,* vol. 910227, p. 15, 1991.

[17] J. D. Naber, D. L. Siebers, S. D. Julio and C. K. Westbrook, "Effects of natural gas composition on ignition delay under diesel conditions," *Combustion and Flame, vol. 99,* pp. 192-200, 1994.

[18] G. S. Settles, Schlieren and Schadowgraph Techniques, New York: Springer, 2001.

[19] C. Chartier, "Optical investigations of spray processes in diesel engines," *SAE International,* p. 22, 2010.

[20] J. Heywood, "Internal combustion engines fundamentals," in *Internal combustion engines fundamentals Vol 2*, 1988, pp. 638-640.

[21] D. Schmidradler, "Temperaturmessung im Verbrennungsraum eines diesel motors mittels RGB-kamera," in *DISSERTATION*, Vienna, Schmidradle Technischen Universität Wien, 1999, pp. 43-50.

[22] O. Andersen and J. E. Weinbach, "Residual animal fat and fish for bio diesel production. potentials in Norway," *Biomass and Bioenergy,* pp. 1183-1188, 2010.

[23] C. Baumgarten, Mixture Formation in Internal Combustion Engines, Hannover: Springer, 2006.

[24] M. S. Graboski and R. L. McCormick, "Combustion of Fat and Vegetable Oil Derived Fuels in Diesel Engines," *Pergamon,* vol. Golden, 1998.

[25] J. Pullen and K. Saeed, "An overview of biodiesel oxidation stability," *Renewable and Sustainable Energy Reviews,* vol. 16, pp. 5924-5950, 2012.

[26] M. S. a. A. Leipertz, “Influence of Nozzle Hole Geometry, Rail Pressure and Pre-Injection on Injection, Vaporisation and Combustion in a Single-Cylinder Transparent Passenger Car Common Rail Engine,” *SAE TECHNICAL,* vol. 2665, pp. 1-10, 2002-01.

[27] V. Schwarz, G. Koenig, P. Dittrich and K. Binder, "Analysis of mixture formation, combustion and pollutant formation in hd diesel engines using modern optical diagnostics and numerical simulation," *SAE Interantional,* p. No. 3647, 1999.

[28] P. Soltic, D. Edenhauser and T. Thurnheer, "Experimental investigation of mineral diesel fuel, GTL fuel rapeseed oil combustion in a heavy duty on-road engine with exhaust gas," *Fuel Vol. 88,* pp. 1-88, 2008.

[29] E. Mancaruso and B. M. Vaglieco, "Premixed combustion of GTL and RME fuels in single cylinder research engine," *Applied Energy, vol. 91,* pp. 385-394, 2012.

[30] D. L. Siebers and B. S. Higgins, "Effects of Injector Conditions on the Flame Lift Off Length of DI Diesel

Sprays," *Sandia National Laboratories,* 2000.

[31] G. Stiesch, Modeling Spray and Combustion Process, Hannover: Springer, 2003.

Acknowledgments

The authors gratefully thank Per Magne Einang (Research Director at Marintek), the injector producer L'Orange for the financial and wealth of ideas to support this project. Thank also goes to Roger Røstad, head of Processing at ScanBio, for providing the crude fish oil and Marine Ingredients for providing the FAEE.

Definitions/Abbreviations

CVPC	Constant Volume Pre- combustion Cell
PC	**Pre-Combustion**
FAEE	Fatty Acid Ethyl Ester
MGO	Marine gas oil
ROHR	Rate of Heat Release
LHV	Lower heat value
MFB	Mass fraction Burned
ROHR	Rate of Heat Release
BEMP	Brake Mean Effective Pressure
CFO	Crude Fish Oil